

# Controllable synthesis of PbI<sub>2</sub> nanocrystals via a surfactant-assisted hydrothermal route

Gangqiang Zhu · Peng Liu · Mirabbos Hojamberdiev · Jian-ping Zhou · Xijin Huang · Bo Feng · Rong Yang

Received: 24 June 2009 / Accepted: 1 September 2009 / Published online: 19 September 2009  
© Springer-Verlag 2009

**Abstract** PbI<sub>2</sub> nanostructures were successfully prepared via a surfactant-assisted hydrothermal method at a low temperature of 100°C for 8 h. Polyvinyl pyrrolidone (PVP) and cetyltrimethylammonium bromide (CTAB) were used as surfactants. The resulting products were characterized by X-ray diffraction (XRD), scanning electron microscopy (SEM), transmission electron microscopy (TEM), and UV-vis spectroscopy. It was found that the formation of PbI<sub>2</sub> nanostructures with various morphologies could be well controlled by the adjustment of the pH of the synthesis solution, selection of suitable surfactant, and the amount of the desired surfactant. UV-vis absorption results showed an apparent shift of the band gap energy of the PbI<sub>2</sub> nanoparticles relative to that of the bulk.

**PACS** 62.23.Hj · 73.22.-f · 78.22.Fd · 81.20.Ka · 81.16.Be · 91.67.JK

## 1 Introduction

It is generally believed that the properties of nanomaterials depend not only on their chemical compositions, but also on their structures, including phases, sizes, shapes, size distribution and the dimensionality [1, 2]. Controlling anisotropic

inorganic materials at the mesoscopic level is one of the most challenging issues presently faced by materials scientists. In the past two decades, a variety of nanostructures have been extensively developed by different synthesizing processes [1, 3, 4].

Lead iodide (PbI<sub>2</sub>) is an intrinsic wide band gap semiconductor ( $E_g = 2.3\text{--}2.55$  eV) having high molecular weight and high resistivity [5]. So far, lead iodide has been intensively studied owing to its exceptional optical and electrical properties as well as specific technological application for photocell, X-ray and  $\gamma$ -ray detectors [6–8]. As a high-anisotropic semiconductor, PbI<sub>2</sub> has a CdI<sub>2</sub> type of layered structure, with repeat unit of hexagonally closed-packed layer of Pb<sup>2+</sup> sandwiched between two layers of I<sup>−</sup> in the crystal [9]. In general, PbI<sub>2</sub> is expected to grow with high-anisotropic low-dimensional nanostructures perpendicular to the *c*-axis and the stacking of weakly bound layers under a suitable synthesis conditions.

Recently, a number of research works have been reported on the synthesis of the PbI<sub>2</sub> nano- and microstructures, and films by chemical and physical methods. For example, colloidal [9], sol-gel [10], reverse micelles [11], vapor deposition [12] and hydrothermal [13–15] techniques were employed for growth of the PbI<sub>2</sub> nano- and microstructures. Among these methods, the hydrothermal method is an attractive route to prepare the inorganic solids with narrow particle size distribution and well-controlled morphologies through one-step procedure at lower temperature [3]. In this work, we considered to fabricate the PbI<sub>2</sub> nanostructures via a simple hydrothermal method assisted with surfactants at the temperature of 100°C for 8 h. The effects of the pH of the synthesis solution, surfactant type, and the amount of the surfactant on the morphologies of lead iodide products were systematically investigated. The understanding of the

G. Zhu (✉) · P. Liu · J.-P. Zhou · X. Huang · B. Feng · R. Yang  
School of Physics and Information Technology,  
Shaanxi Normal University, Xi'an, 710062, P.R. China  
e-mail: [zgq2006@snnu.edu.cn](mailto:zgq2006@snnu.edu.cn)  
Fax: +86-29-85303823

M. Hojamberdiev  
Shaanxi Key Laboratory of Nano-materials and Technology,  
Xi'an University of Architecture and Technology, Xi'an, 710055,  
P.R. China

role of these parameters is of great importance for us to further exploit the growth of the  $\text{PbI}_2$  nanostructures with well-controlled morphologies.

## 2 Experimental

### 2.1 Synthesis

Analytical grade lead acetate ( $\text{Pb}(\text{CH}_3\text{CO}_2)_2$ ), potassium iodide (KI), CTAB and PVP ( $M = 40000$ ) were used as precursors, purchased from Shanghai Chemical Ltd Corp. All the chemicals were used without further purification. Deionized water was used throughout. In a typical synthesis, 0.9531 g of  $\text{Pb}(\text{CH}_3\text{CO}_2)_2$  was dissolved in a 10 ml diluted acetic acid, and 0.10 g of CTAB (or 0.06 g PVP) was added into the solution; 0.4193 g KI was dissolved in 5 ml distilled water. Subsequently, the KI solution was slowly dropped into the  $\text{Pb}(\text{CH}_3\text{CO}_2)_2$  solution under vigorous stirring, and a yellow-colored precursor was obtained. 15 ml deionized water was added into the yellow-colored precursor and under vigorous stirring for 10 min. Finally, the amorphous precursor of 30 ml was transferred into the Teflon-lined autoclave and heated at 100°C for 8 h. After the system was cooled down to room temperature, the final products was rinsed with distilled water several times, and dried at 60°C for 4 h.

### 2.2 Characterization

The phase purity and crystallinity of the as-prepared products were characterized by X-ray diffraction (XRD, Model D/Max2550VB+/PC, Rigaku, Japan) at a scanning rate of 5°  $\text{min}^{-1}$  in the 2 $\theta$  range from 10° to 60°, with  $\text{CuK}\alpha$  radiation ( $\lambda = 1.5406 \text{ \AA}$ ) at 40 kV and 50 mA. Scanning electron microscopy (SEM) images of the samples were taken with a FEI Quanta 200 (The Netherlands) equipped with X-ray energy dispersive spectrometer (EDS). Transmission electron microscopy (TEM), selected area electron diffraction pattern (SAED), and high-resolution transmission electron microscopy (HRTEM) observations were performed on an electron microscope (Model JEM-2100, JEOL, Japan) with an accelerating voltage of 200 kV. Optical adsorption spectra were obtained at room temperature by a UV-visible spectrophotometer (Lambda 950, Perkin-Elmer, USA) in the range of 350–600 nm.

## 3 Results and discussion

The composition and phase purity of the as-prepared products were first analyzed by an X-ray diffraction. The XRD patterns of the  $\text{PbI}_2$  powders synthesized at 100°C for 8 h

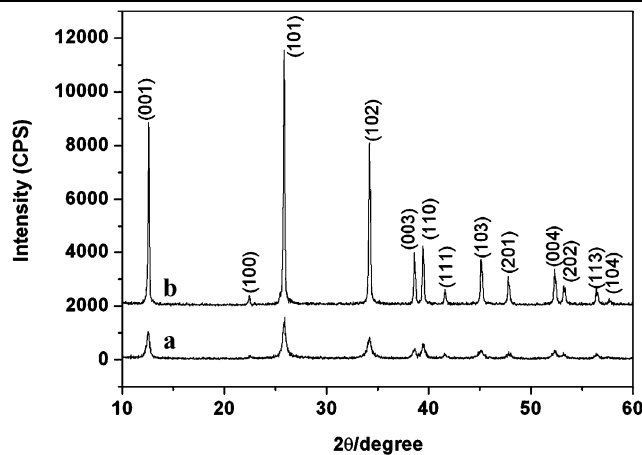


**Fig. 1** XRD patterns of the  $\text{PbI}_2$  powders synthesized via hydrothermal method with PVP (a) and CTAB (b) at 100°C for 8 h

with assistance of CTAB and PVP are shown in Fig. 1. All the peaks in Fig. 1 can be readily indexed to a pure hexagonal structure (JCPDS Card No. 79-0803) with space group of  $P-3m1(164)$ , corresponding to the bulk  $\text{PbI}_2$ . The strong and sharp diffraction peaks in Fig. 1a indicate high crystallinity of the  $\text{PbI}_2$  powders. The calculated cell parameters of the as-synthesized  $\text{PbI}_2$  crystals are  $a = b = 4.568 \text{ \AA}$  and  $c = 6.991 \text{ \AA}$ , which are well compatible with the reported data ( $a = b = 4.557 \text{ \AA}$ ,  $c = 6.979 \text{ \AA}$ ). Furthermore, the wide peaks indicating the average crystalline size of the sample synthesized with PVP are relatively small. Using the Scherrer formula, the estimated crystalline size is about 100 nm, which is consistent with the results obtained from transmission electron microscopy, as shown in Fig. 2a.

Size and morphology information of the  $\text{PbI}_2$  powders obtained from scanning electron microscopy (SEM) and transmission electron microscopy (TEM) is represented in Fig. 2 and Fig. 3. Figure 2a–b shows low- and high-magnification TEM images of the as-prepared  $\text{PbI}_2$  powders synthesized with 0.06 g PVP at 100°C for 8 h. It can be seen that the as-prepared powder consists of large-scale nanoplates with a diameter in the range of 20–150 nm. A single nanoplate with a diameter about 60 nm was shown in Fig. 2c and the lattice fringe of 0.70 nm in the HRTEM image (inset in Fig. 2c) agrees well with the (001) lattice plane. Twinned nanoplates with a clear interface can also be observed in the products, as shown in Fig. 2b. Further insight into the twinning nanoplate was gained by HRTEM observation (Fig. 2d). The lattice fringe of 0.261 nm in the observed region A agrees well with the (102) lattice plane and the lattice fringe of 0.261 nm and 0.234 nm in the observed region B agree well with the (102) and (003) lattice planes, respectively. The SAED pattern shown inset in Fig. 2d can also be indexed to the hexagonal structure  $\text{PbI}_2$ . As the surfactant of PVP is replaced by CTAB, large-scale uniform  $\text{PbI}_2$  nanorods were obtained (Figs. 3a–b), in

**Fig. 2** Low- (a) and high- (b) magnification TEM, (c) single nanoplate and (d) twinned nanoplate HRTEM images of the  $\text{PbI}_2$  synthesized via a hydrothermal method with PVP

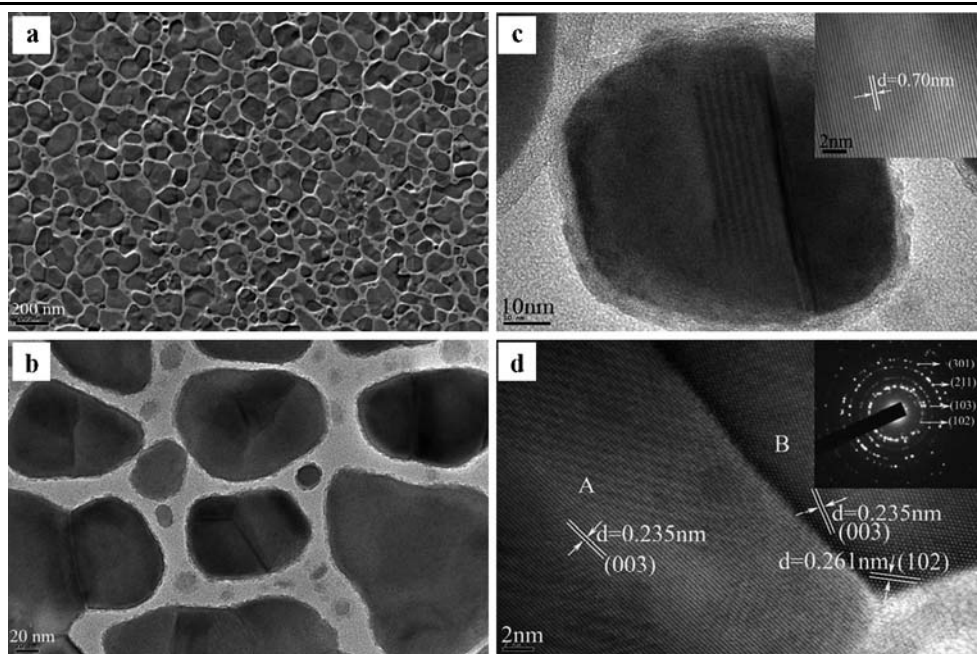
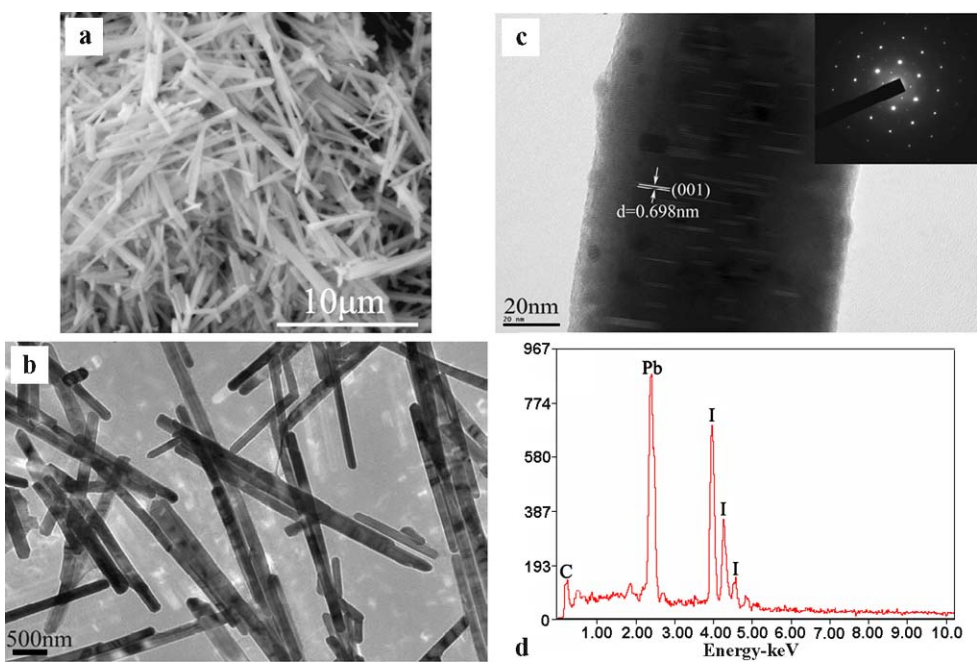


**Fig. 3** SEM (a), TEM (b), HRTEM (c) images and EDS pattern (d) of the  $\text{PbI}_2$  nanorods synthesized via hydrothermal method with CTAB



which the widths of the nanorods are about 500 nm and the lengths in the range of 3–12  $\mu\text{m}$ . To understand the preferential orientation growth,  $\text{PbI}_2$  nanorods have been further studied using HRTEM, and the results are shown in Fig. 3c. HRTEM images indicated that  $\text{PbI}_2$  nanorods existed as a single-crystal structure, the lattice fringe of 0.698 nm in the observed nano-crystallites agrees well with the (001) lattice plane, indicating the nanorod with preferring growth of the *c*-axis. It is in accordance with the SAED results (inset in Fig. 3c). According to X-ray energy dispersive spectrometer (EDS) results, the molar ratio of Pb:I obtained from the peak area (Fig. 3d) is 1:1.95, which is close to 1:2, giving a possible composition of  $\text{PbI}_2$ .

In order to find the effect of the pH value on the phase structures of the final products, the pH values were varied from 3 to 12 using acetic acid. It was found that the pH values of the reaction solution have great effect on the phase structures of the final products prepared at 100°C for 8 h with CTAB. Pure hexagonal phase  $\text{PbI}_2$  could be obtained as the pH values in the range of 3–6 (Fig. 4a–c). When the

pH values of the reaction solution  $\geq 7$ , pure Pb(OH)I with an orthorhombic structure (JCPDS: 75-1177) was obtained (Fig. 4d–e).

We further emphasized the importance of the surfactants (CTAB or PVP) in the formation of PbI<sub>2</sub> microstructures. The experimental results showed that the amount of CTAB

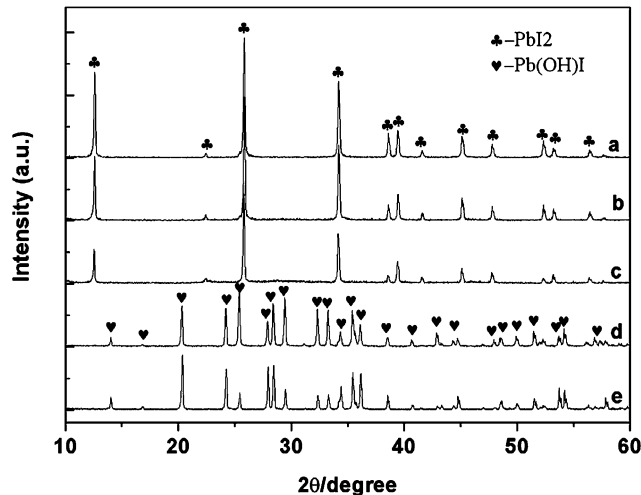


**Fig. 4** XRD patterns of the PbI<sub>2</sub> powders synthesized via the hydrothermal method with CTAB in different pH: 3 (a), 5 (b), 6 (c), 7 (d), and 12 (e)

**Fig. 5** SEM images of the PbI<sub>2</sub> powders synthesized via the hydrothermal method with different amounts of CTAB: 0 g (a), 0.04 g (b), 0.06 g (c), and 0.10 g (d)

in the synthesis solution have great effect on the morphology of the final products. By adjusting the amount of CTAB, PbI<sub>2</sub> with different morphologies can be obtained accordingly, and the corresponding SEM images are illustrated in Fig. 5. In the absence of CTAB in the synthesizing system, large-scale PbI<sub>2</sub> microplates with a diameter of about 10  $\mu\text{m}$  were obtained (Fig. 5a). When 0.04 g CTAB is added to the synthesizing system, PbI<sub>2</sub> microplates with a diameter in the range of 3–6  $\mu\text{m}$  and some nanorods with a diameter in the range of 300–1000 nm were obtained (Fig. 5b). Further increase of the amount of CTAB to 0.08 g led to the formation of many PbI<sub>2</sub> nanorods with a diameter in the range of 300–1000 nm and a few microplates with a diameter of about 3  $\mu\text{m}$  (Fig. 5c). When the amount of 0.10 g CTAB is introduced, the as-synthesized nanorods have a diameter of about 500 nm and a length in the range of 3–15  $\mu\text{m}$  (Fig. 5d). Fewer plate-like products were found in the final products. As is well known, PVP is an ionic compound, which ionizes completely in water. In the synthetic procedure of nano-materials or microstructures, PVP is used as a capping agent. So far, PVP has been systematically studied in the synthesis of different morphology nano-materials [16–18]. And the amount of PVP in the synthesizing system has also effects on the size and morphology of the final products in this work. When the amount of PVP is increased to 0.08 g, as-synthesized nanoplates with a diam-

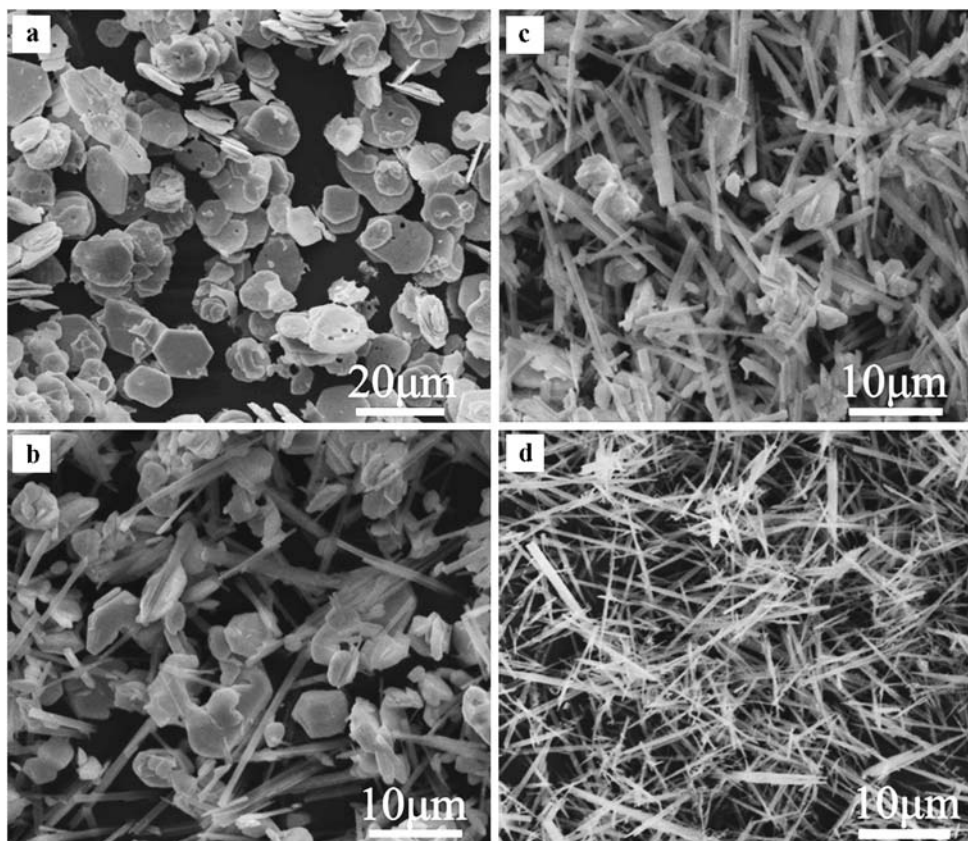


**Fig. 6** SEM images of the  $\text{PbI}_2$  powders synthesized via the hydrothermal method with different amounts of PVP: 0.08 g (a), 0.10 g (b), and 0.12 g (c, d)

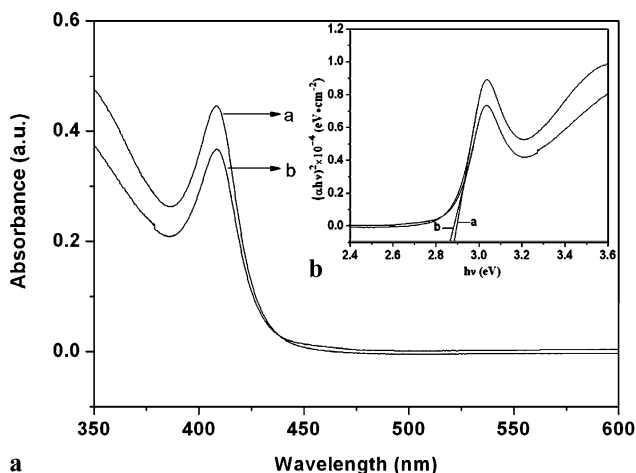
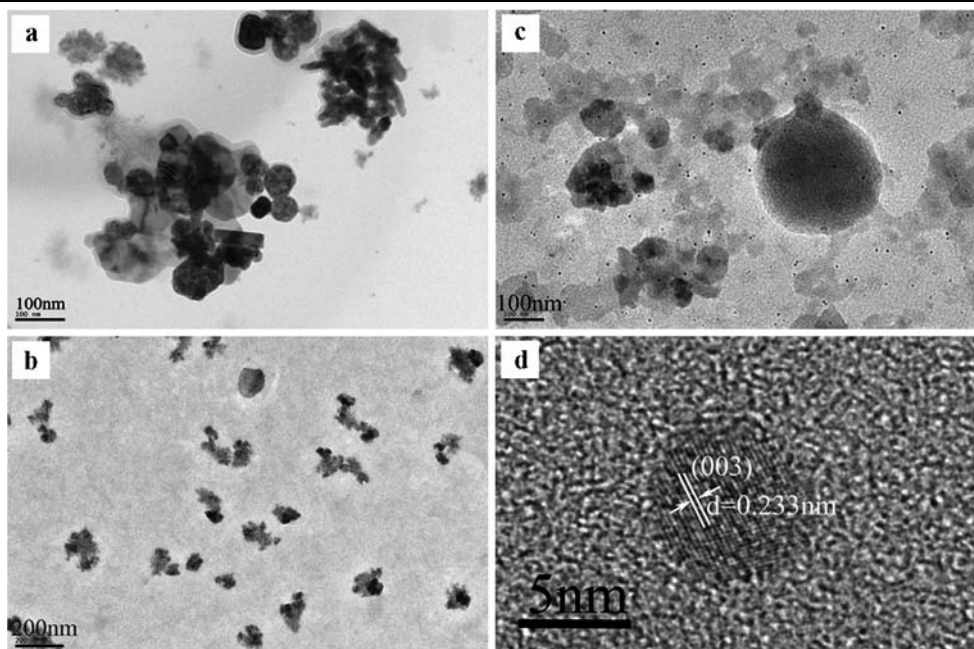


**Fig. 7** UV-vis spectra (a) and plot of  $(\alpha h v)^2$  versus  $h v$  (b) of the  $\text{PbI}_2$  nanoplates (a) and nanorods (b) via the hydrothermal method

eter in the range of 50–100 nm were obtained as shown in Fig. 6a. As the amounts of PVP further increased to 0.10 g, lots of  $\text{PbI}_2$  particles with an irregular shape of about 50 nm were obtained (Fig. 6b). Figure 6c shows that the sample synthesized with 0.12 g PVP possesses a lot of nanodots with a diameter in the range of 5–10 nm. Figure 6d shows a HRTEM image of a single nanodot with a diameter of about 5 nm. When further increasing the amount of PVP in the synthesizing system, products with an unknown structure were obtained. In the synthesis system, PVP molecules attach on the surface of the nanoparticles, which could form a shell surrounding the particles to prevent  $\text{PbI}_2$  particles from being aggregated into larger particles. So no large size par-

ticles could be found in the final products when a suitable amount of PVP was added into the reaction solution.

Figure 7a shows the UV-vis optical absorption spectra of the  $\text{PbI}_2$  nanorods and nanoplates. The optical data are analyzed at the near absorption edge, using the equation  $\alpha = k(hv - E_g)^{n/2} / hv$  are shown in Fig. 7b, where  $k$  and  $n$  are constants and  $E_g$  is the band gap of the semiconductor. The value of  $n$  is equal to 1 for direct transition materials, including  $\text{PbI}_2$ . The plot of  $(\alpha h v)^2$  versus  $h v$  gives an  $E_g$  value at ca. 2.86 and 2.88 eV, which shift to a higher energy in comparison with a typical direct band gap (2.5 eV) of bulk  $\text{PbI}_2$  crystal.

#### 4 Conclusion

High crystalline  $\text{PbI}_2$  nanorods, nanoplates and nanodots were successfully prepared by a simple hydrothermal method at the temperature of 100°C for 8 h. The results show that the pH of the synthesis solution, surfactant type, and the amount of the surfactant are important for the formation of the  $\text{PbI}_2$  nanostructures with various morphologies. UV-vis spectra results confirmed the appearance of a shift of the  $\text{PbI}_2$  nanostructures, relating to the bulk  $\text{PbI}_2$ . The understanding of the role of these parameters is of great importance for us to further exploit the growth of the  $\text{PbI}_2$  nanostructures with well-controlled morphologies.

#### References

- B.L. Cushing, V.L. Kolesnichenko, C.J. O'Connor, Chem. Rev. **104**, 3893 (2004)

2. N. Pinna, M. Niederberger, *Angew. Chem. Int. Ed.* **47**, 5292 (2008)
3. K. Byrappa, T. Adschari, *Prog. Cryst. Growth. Ch.* **53**, 117 (2007)
4. C. Burda, X.B. Chen, R. Narayanan, M.A. El-Sayed, *Chem. Rev.* **105**, 1025 (2005)
5. T. Unagami, *J. Electrochem. Soc.* **146**, 3110 (1999)
6. T.E. Schlesinger, R.B. James, M. Schieber, J. Toney, J.M. Van Scyoc, L. Salary, H. Hermon, J. Lund, A. Burger, K.-T. Chen, E. Cross, E. Soria, K. Shah, M. Squillante, H. Yoon, M. Goorsky, *Nucl. Instr. Meth. A* **380**, 193 (1996)
7. M.A. George, M. Azoulay, H.N. Jayatirtha, Y. Biao, A. Burger, W.E. Collins, E. Silberman, *J. Crystal. Growth.* **137**, 299 (1994)
8. Y.C. Chang, R.B. James, *Phys. Rev. B* **55**, 8219 (1997)
9. K. Mallik, T.S. Dhami, *Phys. Rev. B* **58**, 13055 (1998)
10. E. Lifshitz, M. Yassen, L. Bykov, I. Dag, *J. Lumin.* **70**, 421 (1996)
11. G.K. Kasi, N.R. Dollahon, T.S. Ahmadi, *J. Phys. D: Appl. Phys.* **40**, 1778 (2007)
12. M. Schieber, N. Zamoshchik, O. Khakhan, A. Zuck, *J. Crystal. Growth.* **310**, 3168 (2008)
13. D.K. Ma, W. Zhang, R. Zhang, M. Zhang, G.C. Xi, Y.T. Qian, *J. Nanosci. Nanotechnol.* **5**, 810 (2005)
14. Z. Zheng, A.R. Liu, S.M. Wang, Y. Wang, Z.S. Li, W.M. Lau, L.Z. Zhang, *J. Mater. Chem.* **15**, 4555 (2005)
15. Z. Zheng, S.M. Wang, D.P. Li, A.R. Liu, B.J. Huang, H.X. Zhao, L.Z. Zhang, *J. Crystal. Growth.* **308**, 398 (2007)
16. Y.L. Wang, M. Guo, M. Zhang, X.D. Wang, *Scr. Mater.* **61**, 234 (2009)
17. A.P. Zhang, J.Z. Zhang, *Spectrochim. Acta Part A* **73**, 336 (2009)
18. S. Phoka, P. Laokul, E. Swatsitang, V. Promarak, S. Seraphin, S. Maensiri, *Mater. Chem. Phys.* **115**, 423 (2009)